Proceedings of the 17th World Congress
The International Federation of Automatic Control
Seoul, Korea, July 6-11, 2008

Design of Piecewise Linear LQ Control for Linear Systems with Rate Saturations Using LMI Optimization

Noriyuki Akasaka *

* *Kurume National College of Technology, 1-1-1 Komorino,Kurume-City,Fukuoka Japan (Tel: +81-942-35-9391; e-mail: akasaka@kurume-nct.ac.jp).*

Abstract: A model of the servomechanism used for high-powered actuators in mechanical systems consists of a position feedback loop around the cascade connection of a memoryless saturation function with an integrator with a large time constant. The saturation function in the servomechanism has a linear high gain characteristics for a small input and so the equivalent time constant of the actuator servomechanism becomes small. As the input to the saturation function becomes larger than the linear range for a drastic control demand, the output of the saturation function becomes constant irrespective of the input magnitude and the actuator response has a rate saturation determined by the large time constant of the integrator and so the time lag of the actuator response behind the demand results in the actual plant input much different from the demand and the plant may exhibit an undesirable behavior of the system. Therefore in this paper we consider a control method for a system with rate saturations in the actuator servomechanisms to keep stable by switching the controller gain according to the input magnitudes to the saturation functions so that the inputs to the saturation functions are controlled within the permissible maximum absolute values which are decided according to each level of LQ controller gain groups determined beforehand to ensure the local absolute stability of the total system whose conditions are expressed as a linear matrix inequalities optimization problem by introducing a Lure-type Lyapunov function. In a piecewise linear control the switching function selects a controller gain group by on-line monitoring the inputs to the saturation functions in the actuator servomechanisms. The effectiveness of the design method is illustrated with a practical example of dynamic positioning(DP) system.

1. INTRODUCTION

Various procedures have been developed for the design of controllers that account for the amplitude and rate saturations of actuators. In Edwards et al. (1999), Hippe et al. (1999), Kapoor et al. (1998) and Kothare et al. (1994) the basic procedure of anti-windup design methods is to design a controller first ignoring the control input saturation and then to add an anti-windup compensator so that the effect of the control input saturation on closed-loop performance is minimized. Another stability analysis and/or synthesis methods for systems with magnitude and rate saturations have been developed in Hindi et al. (1998), Khalil (2002), Kiyama et al. (2000), Kothare et al. (1999), Pare et al. (1998) and Pittet et al. (1997). The basic idea is the notion of positively invariant set in Blanchini (1999) and the Lyapunov analysis, and the circle and the Popov criteria are used within the framework of linear matrix inequalities(LMIs).

On the other hand, gain scheduling controllers have been developed as a design method for nonlinear control in Lawrence et al. (1995) and Rugh et al. (2000). In the gain-scheduled controller which includes an integral control, the velocity algorithm has to be used so that the linearization property holds in Kaminer et al. (1995). In Wredenhagen et al. (1994), a piecewise linear control law based on LQ theory is derived which raises an LQ gain as the controlled error converges towards the origin. The notion of gain switching function is introduced, which gives the successive positively invariant set and the highest LQ gain possible in the presence of the input bounds.

A model of the servomechanism used for high-powered actuators in mechanical systems consists of a position feedback loop around the cascade connection of a memoryless saturation function with an integrator with a large time constant. The saturation function in the servomechanism has a linear high gain characteristics for a small input which is the error between the actuator demand from the controller and the actual position value of the actuator and so the equivalent time constant of the actuator servomechanism becomes small regardless of the large time constant of the integrator and the time lag of the actuator response behind the actuator demand is negligible. As the input to the saturation function becomes larger than the linear range for a drastic actuator demand, the output of the saturation function becomes constant irrespective of the input magnitude and the actuator response has a rate saturation determined by the large time constant of the integrator and so the time lag of the actuator response behind the demand results in the actual plant input much different from the controller demand and the plant may exhibit an undesirable behavior such as an excessive overshoot and further the control system may become unstable. Therefore in this paper we consider a control method for a system with rate saturations in the actuator servomechanisms to keep stable by realizing the controller gain switching according to the input magnitudes to the saturation functions so that the inputs to the saturation functions are controlled within the permissible maximum absolute values which are decided to ensure the local absolute stability of the total system . In design procedures of the control method firstly a set of LQ gain groups for the linear dynamical system ignoring

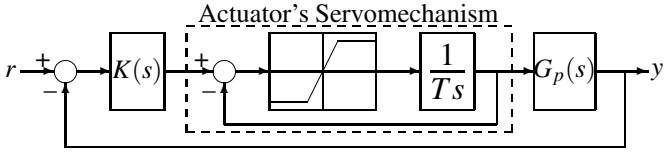

Fig. 1. Block diagram of a total system

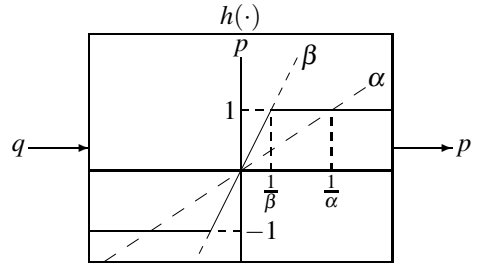

Fig. 2. Saturation function $h(\cdot)$

the dynamics of actuator servomechanism is computed off-line by changing the control weight of the quadratic performance criterion stepwise under the fixed state weight. Secondly the block diagram of a total system including the actuator servomechanisms is redrawn as the feedback connection of a linear dynamical system and a decoupled block of multiple saturation functions with magnitudes ± 1 treated as locally sector bounded nonlinearities. Then the permissible maximum absolute input values to the nonlinearities are decided according to each level of LQ controller gain groups determined above, by introducing a Lure-type Lyapunov function to the redrawned block diagram to ensure the local absolute stability of the total system whose conditions are expressed as an LMIs optimization problem in Boyd et al. (1994). In control procedures a controller gain switching function is introduced to realize a piecewise linear control(PLC) law which always gets a local absolute stability of the total system. The switching function selects a controller gain group by on-line monitoring the inputs to the saturation functions in the actuator servomechanisms. The effectiveness of the design method is illustrated with a practical example of dynamic positioning(DP) system which holds the position and heading of a ship under wind disturbances by controlled thrusters.

2. DESIGN OF PIECEWISE LINEAR LQ CONTROL

2.1 A Set of LQ Gain

Fig.1 shows a block diagram of a system consisting of a controller dynamics $K(s)$, a dynamics of an actuator servomechanism and a plant dynamics $G_p(s)$. When the controller gain is determined based on LQ theory, we ignore the dynamics of actuator servomechanisms and assume that all outputs can be measured. By changing the control weight of the quadratic performance criterion stepwise under the fixed state weight, a set of LQ gain groups is decided.

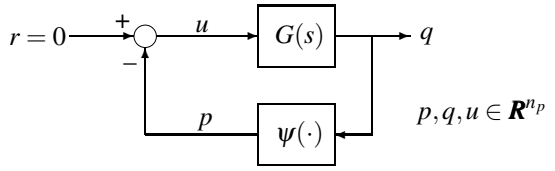

Fig. 3. Feedback connection of a linear dynamic system and multiple saturation functions

2.2 Permissible Sector Conditions of Saturation Functions

Fig.2 shows one of saturation functions $h(\cdot)$ with the magnitudes ± 1 in the actuator servomechanism in Fig.1, by scaling the input and output of the saturator. The saturator $h(\cdot)$ has a linear gain β in the input range of $|q| \le 1/\beta$. If the absolute value of the input q to the saturator $h(\cdot)$ is constrained less than $1/\alpha$, the sector condition $h \in [\alpha\ \beta]$ is satisfied locally. The objective of this paper is to determine the maximum absolute values $1/\alpha$ of inputs to the multiple saturation functions simultaneously as reciprocals of the minimum sector bounds α to ensure the local absolute stability of a total system. Firstly we redraw the block diagram of the total system as a feedback connection of a linear dynamical system $G(s)$ and a decoupled block of multiple saturation nonlinearities $\psi(\cdot)$ as shown in Fig.3 in Khalil (2002) and Boyd et al. (1994). $\psi(\cdot)$ is assumed to be $\mathrm{diag}(\psi_1(\cdot)\cdots\psi_{n_p}(\cdot))$ and has sector conditions $\psi_i \in [\alpha_i\ \ \beta_i](1 \le i \le n_p)$. As it is very difficult to decide the minimum sector bounds $\alpha_i (1 \le i \le n_p)$ of the original multiple saturation functions $\psi(\cdot)$ simultaneously by checking the condition of positive realness of the loop-transformed linear dynamical system as in Akasaka (2006), we use the Lyapunov analysis to accomplish the objective above by introducing a Lure-type Lyapunov function and derive the LMIs associated with the original system shown in Fig.3 as indicated in the chapter 8 Notes of Boyd et al. (1994).

Consider the linear system $G(s)$ with a decoupled block of multiple saturation functions in Fig.3:

$$\dot{x} = Ax + Bu, \tag{1}$$
$$q = Cx, \tag{2}$$
$$u_i = -p_i, \quad p_i = \psi_i(q_i)\ \ (1 \le i \le n_p) \tag{3}$$

where $x \in \boldsymbol{R}^{n_x}, u \in \boldsymbol{R}^{n_p}, p \in \boldsymbol{R}^{n_p}$ and $q \in \boldsymbol{R}^{n_p}$. $\psi(\cdot)$ denotes the decoupled block of saturation functions with the magnitudes ± 1 and defined on a scalar $q_i \in \boldsymbol{R}^1 (1 \le i \le n_p)$ by

$$\psi_i(q_i) \triangleq \begin{cases} 1 & q_i > 1/\beta_i, \\ q_i & |q_i| \le 1/\beta_i \quad (\beta_i > 0), \\ -1 & q_i < -1/\beta_i, \end{cases} \tag{4}$$

and on a vector $q = (q_1, \cdots, q_{n_p})$ by

$$\psi(q) \triangleq (\psi_1(q_1), \cdots, \psi_{n_p}(q_{n_p})). \tag{5}$$

If the absolute value of the input q_i to the saturator $\psi_i(\cdot)$ is assumed to be constrained less than or equal to $1/\alpha_i > 0$, the function $\psi_i(\cdot)$ satisfy the sector condition $\psi_i \in [\alpha_i\ \beta_i]$:

$$\alpha_i q_i^2 \le q_i \psi_i(q_i) \le \beta_i q_i^2 \quad \text{for all}\ \ q_i \in \boldsymbol{R}^1\ (1 \le i \le n_p), \tag{6}$$
$$\alpha_i > 0\ (1 \le i \le n_p). \tag{7}$$

The sector conditions (6) can be rewritten as

$$(\psi - K_1 q)^T (\psi - K_2 q) \le 0, \tag{8}$$
$$K_1 = \mathrm{diag}(\alpha_1, \cdots, \alpha_{n_p}), \quad K_2 = \mathrm{diag}(\beta_1, \cdots, \beta_{n_p}). \tag{9}$$

The Lure-type Lyapunov function $V(x)$ is used and given as

$$V(x) = x^T P x + 2\sum_{i=1}^{n_p} \gamma_i \int_0^{q_i} (\psi_i(\sigma) - \alpha_i \sigma) d\sigma. \tag{10}$$

The matrix P and the scalars γ_i are the data describing the Lyapunov function and the following conditions are required.

$$P > 0, \tag{11}$$
$$\gamma_i \ge 0 \quad (1 \le i \le n_p). \tag{12}$$

The time derivative $\dot{V}(x)$ is given by

$$\dot{V}(x) = \dot{x}^T P x + x^T P \dot{x} + 2\sum_{i=1}^{n_p} \gamma_i (\psi_i(q_i) - \alpha_i q_i) \dot{q}_i. \tag{13}$$

Using (1),(2) and (3), (13) is given by

$$\dot{V}(x) = \begin{bmatrix} x \\ u \end{bmatrix}^T \begin{bmatrix} P_{11} & P_{12} \\ P_{12}^T & P_{22} \end{bmatrix} \begin{bmatrix} x \\ u \end{bmatrix}, \tag{14}$$

$$\left.\begin{array}{l} P_{11} = A^T P + PA - C^T \Gamma K_1 CA - A^T C^T K_1 \Gamma C, \\ P_{12} = PB - A^T C^T \Gamma - C^T \Gamma K_1 CB, \\ P_{22} = -\Gamma CB - B^T C^T \Gamma, \\ \Gamma = \mathrm{diag}(\gamma_1, \cdots, \gamma_{n_p}). \end{array}\right\} \tag{15}$$

From (14) the stability condition is given by

$$\begin{bmatrix} P_{11} & P_{12} \\ P_{12}^T & P_{22} \end{bmatrix} < 0. \tag{16}$$

Using (2) and (3), (8) is given by

$$\begin{bmatrix} x \\ u \end{bmatrix}^T \begin{bmatrix} C^T K_1 K_2 C & C^T (K_1 + K_2)/2 \\ (K_1 + K_2)C/2 & I \end{bmatrix} \begin{bmatrix} x \\ u \end{bmatrix} \le 0. \tag{17}$$

Equation (17) yields

$$\begin{bmatrix} C^T K_1 K_2 C & C^T (K_1 + K_2)/2 \\ (K_1 + K_2)C/2 & I \end{bmatrix} \le 0. \tag{18}$$

The S-procedure in Boyd et al. (1994) yields the following sufficient condition for (16) and (18).

$$\begin{bmatrix} P_{11} & P_{12} \\ P_{12}^T & P_{22} \end{bmatrix} - \lambda \begin{bmatrix} C^T K_1 K_2 C & C^T (K_1 + K_2)/2 \\ (K_1 + K_2)C/2 & I \end{bmatrix} < 0 \tag{19}$$

where $\lambda > 0$ is a scalar variable. Equation (19) yields

$$\begin{bmatrix} \bar{P}_{11} & \bar{P}_{12} \\ \bar{P}_{12}^T & \bar{P}_{22} \end{bmatrix} < 0, \tag{20}$$

$$\left.\begin{array}{l} \bar{P}_{11} = A^T \tilde{P} + \tilde{P}A - C^T \tilde{\Gamma} K_1 CA - A^T C^T K_1 \tilde{\Gamma} C - C^T K_1 K_2 C, \\ \bar{P}_{12} = \tilde{P}B - A^T C^T \tilde{\Gamma} - C^T \tilde{\Gamma} K_1 CB - C^T (K_1 + K_2)/2, \\ \bar{P}_{22} = -\tilde{\Gamma} CB - B^T C^T \tilde{\Gamma} - I, \\ \tilde{P} = P/\lambda, \quad \tilde{\Gamma} = \Gamma/\lambda. \end{array}\right\} \tag{21}$$

The constraint (20) can be rewritten by eliminating the variable $\tilde{\Gamma} K_1$ in Boyd et al. (1994) as

$$\tilde{U}^T \begin{bmatrix} \hat{P}_{11} & \hat{P}_{12} \\ \hat{P}_{12}^T & \bar{P}_{22} \end{bmatrix} \tilde{U} < 0, \qquad \tilde{V}^T \begin{bmatrix} \hat{P}_{11} & \hat{P}_{12} \\ \hat{P}_{12}^T & \bar{P}_{22} \end{bmatrix} \tilde{V} < 0, \tag{22}$$

$$\left.\begin{array}{l} \hat{P}_{11} = A^T \tilde{P} + \tilde{P}A - C^T K_1 K_2 C, \\ \hat{P}_{12} = \tilde{P}B - A^T C^T \tilde{\Gamma} - C^T (K_1 + K_2)/2. \end{array}\right\} \tag{23}$$

$\tilde{U}$ and $\tilde{V}$ are orthogonal complements of $[CA\ CB]^T$ and $[-C\ 0]^T$ respectively. Thus we solve the LMIs optimization problem in the variables $\tilde{P}, \tilde{\Gamma}$ and K_1:

$$\begin{array}{ll} \text{minimize} & \mathrm{trace}(K_1 + c\tilde{\Gamma}) \\ \text{subject to} & (7), (11), (12) \text{ and } (22), \\ & c = \mathrm{diag}(c_1, \cdots, c_{n_p}) \end{array} \tag{24}$$

c is the weighting matrix. The problem (24) can be solved by using the LMI software in Gahinet et al. (1995).

We check to be sure that the solution K_1 obtained by the optimization problem (24) gives the condition of strict positive realness required by the Popov criterion in Khalil (2002). Applying the loop transformations by using the solution K_1 to Fig.3 we can get the dynamical system $\bar{G}(s) = M + (I + s\tilde{\Gamma})G(s)[I + K_1 G(s)]^{-1}$ where $M = (K_2 - K_1)^{-1}$ and we check that the solution K_1 gives the strict positive realness of $\bar{G}(s)$.

3. EXAMPLE

3.1 Block Diagram of DP System

Fig.4 shows the DP system concept and DP system holds the position and heading of a ship under current and wind disturbances by detecting deviations from the references and by controlling the thrust vectors. The horizontal ship motion nonlinear equations are shown in the appendix. Two rotating thrusters of controllable pitch angle propeller are equipped at fore and aft parts of the ship body center line that is, a bow thruster(B/T) and a stern thruster(S/T). The linearized model of ship motions is expressed by the following state equations.

$$\dot{x}_1 = x_2, \tag{25}$$

$$\dot{x}_2 = A_1 x_1 + A_2 x_2 + Bu + d, \tag{26}$$

$$x_1 = \begin{bmatrix} x_0 \\ y_0 \\ \psi \end{bmatrix}, \quad x_2 = \begin{bmatrix} u_a \\ v_a \\ r \end{bmatrix} = \begin{bmatrix} \dot{x}_0 \\ \dot{y}_0 \\ \dot{\psi} \end{bmatrix}, \quad u = \begin{bmatrix} \phi_B \\ \theta_B \\ \phi_S \\ \theta_S \end{bmatrix}, \quad d = \begin{bmatrix} d_1 \\ d_2 \\ d_3 \end{bmatrix} \tag{27}$$

where ϕ_B:B/T propeller pitch angle θ_B:B/T azimuth angle ϕ_S:S/T propeller pitch angle θ_S:S/T azimuth angle d_1, d_2: acceleration components in x_0-, y_0-direction by disturbance force d_3:angular acceleration component about z_0-axis by disturbance moment $A_1, A_2 \in \boldsymbol{R}^{3\times3}$: constant matrices $B \in \boldsymbol{R}^{3\times4}$: constant matrix.

DP system realizes effective combinations of B/T and S/T thrust vectors to hold the position and heading of a ship against disturbances. DP controller is fulfilled by PID control and by using the reference vecor $x_{1s}^T = [x_{0s}\ y_{0s}\ \psi_s] = [0\ 0\ 0]$, the control error vector ε is expressed by the following equation

$$\varepsilon = x_{1s} - x_1. \tag{28}$$

The control demand u_d to two thrusters is decided by the following equation.

$$u_d = L_P \varepsilon + L_I \left(\frac{1}{s}\right) \varepsilon + L_D \left(\frac{s}{1 + T_c s}\right) \varepsilon, \tag{29}$$

$$\begin{aligned} u_d^T &= \begin{bmatrix} \dfrac{\phi_{Bd}}{\phi_{max}} & \dfrac{\theta_{Bd}}{\theta_{max}} & \dfrac{\phi_{Sd}}{\phi_{max}} & \dfrac{\theta_{Sd}}{\theta_{max}} \end{bmatrix} \\ &= \begin{bmatrix} \phi'_{Bd} & \theta'_{Bd} & \phi'_{Sd} & \theta'_{Sd} \end{bmatrix} \end{aligned} \tag{30}$$

where L_P, L_I, $L_D \in \boldsymbol{R}^{4\times3}$:PID controller gain matrices, s: Laplace operator T_c:Time constant ϕ_{max}:Maximum propeller pitch angle θ_{max}:Maximum azimuth angle=90^o ϕ_{Bd}:control demand of B/T pitch angle θ_{Bd}:control demand of B/T azimuth angle ϕ_{Sd}:control demand of S/T pitch angle θ_{Sd}:control demand of S/T azimuth angle.

Fig.5 shows the block diagram of DP system consisting of ship motion model(25), (26), PID controller(29) and thrusters' servomechanisms. Eight saturation functions included in thrusters' servomechanisms are named by A1∼D2 as shown in Fig.5. Actual propeller pitch angles ϕ_B, ϕ_S and actual azimuth angles θ_B, θ_S are normalized by the following equations so that the saturation functions have the magnitudes ±1.

$$\phi'_B = \frac{\phi_B}{\phi_{max}}, \quad \theta'_B = \frac{\theta_B}{\theta_{max}}, \quad \phi'_S = \frac{\phi_S}{\phi_{max}}, \quad \theta'_S = \frac{\theta_S}{\theta_{max}}. \tag{31}$$

Signs of ϕ_B, ϕ_S are positive for forward thrusts and negative for backward thrusts. Signs of θ_B, θ_S are positive for thrusts toward starboard and negative for thrusts toward port. By the sign rules above mentioned, normalized variables of thrusters are constrained as follows.

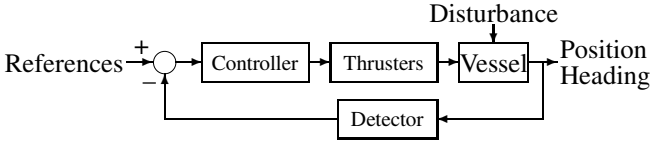

Fig. 4. Concept of dynamic positioning(DP) system

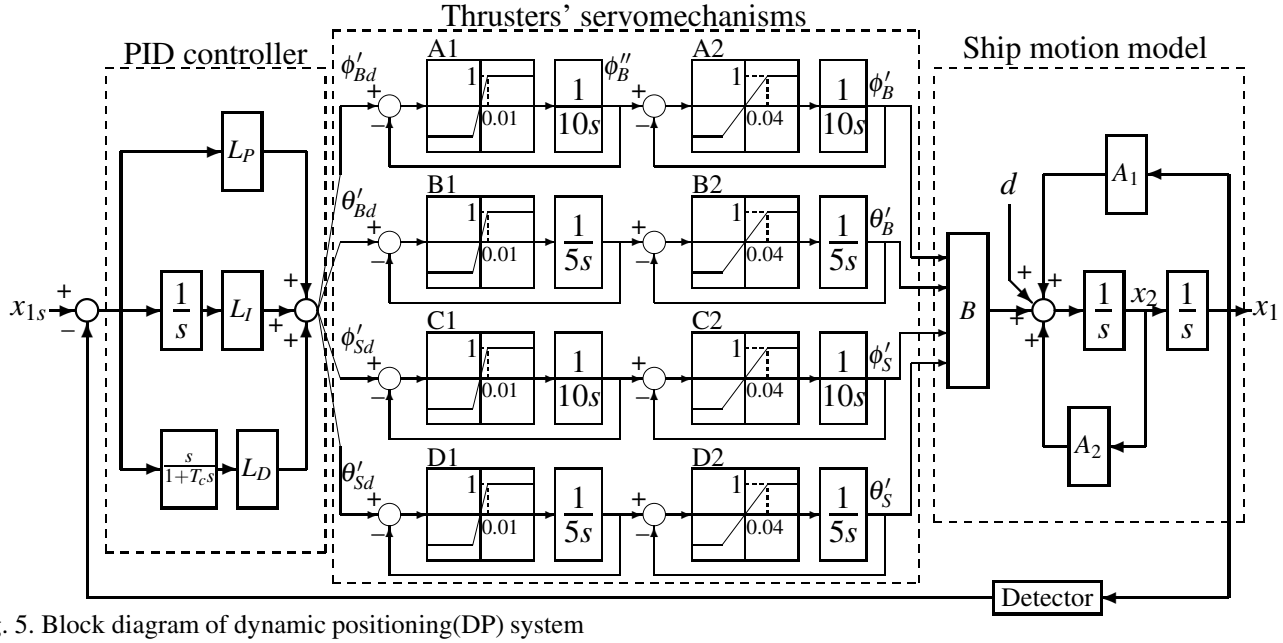

Fig. 5. Block diagram of dynamic positioning(DP) system

Table 1. General data of the ship

Vessel		Thruster	
length	88m	diameter	2.8m
width	19m	speed	200 rpm
draft	4.4m	pitch angle	ahead 24^o
capacity	6080t		astern 21^o
thruster position	34m	max. power	2500PS

$$\left.\begin{array}{ll} -1 \le \phi'_B \le 1, & -2 \le \theta'_B \le 2, \\ -1 \le \phi'_S \le 1, & -2 \le \theta'_S \le 2. \end{array}\right\} \quad (32)$$

Signs of controller gain matrices' elements of L_P, L_I, L_D depend on the quadrant in which the thrust vector stays and so it is necessary to calculate thrust demands after changing the signs of controller gains according to which quadrant the actual thrust vector stays in.

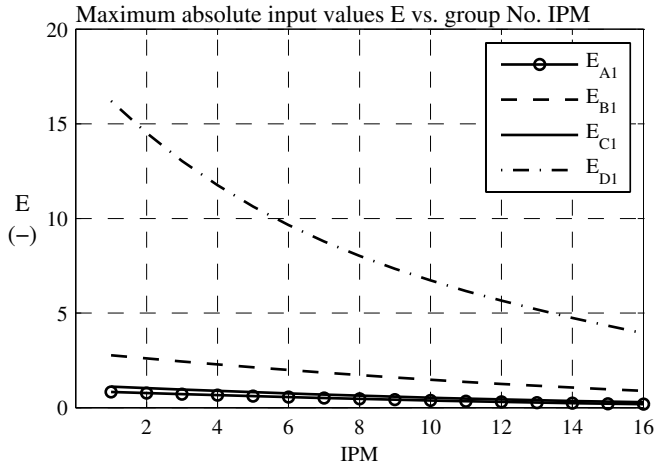

Fig. 6. Maximum absolute input values E

3.2 Design of Piecewise Linear Control for DP System

(1)A Set of PID Controller Gain

General data of the ship to which the design of PLC is applied is shown in Table 1. B/T and S/T have the same data. The linearized model of ship motions is derived from the stationary condition of holding position and heading under the steady wind velocity $U_w = 15$m/sec and wind direction $\psi_w = 30^o$. PID controllers' gains are determined by LQ theory for the linearized model of ship motions ignoring the dynamics of actuator servomechanisms. A set of controller gain matrices L_P, L_I, L_D is composed of 16 groups and the group number of control gain set is expressed by a variable IPM($1 \le$IPM≤ 16) and the larger IPM indicates the larger gain group.

(2)Permissible Sector Conditions of Saturation Functions

Each thruster's servomechanism in Fig.5 consists of a cascade connection of the first servomechanism and the second servomechanism whose integrators have the same time constants and so the input to the saturation function in the second servomechanism is constrained less than the linear range of input to the saturation function for the demand with the maximum rate from the first servomechanism. Therefore the saturation functions A2∼D2 in the second servomechanism are represented by proportional gain elements with the maximum gain and so the dynamics of the second servomechanism is considered to be linear. When we redraw the block diagram in Fig.5 to that in Fig.3, only four saturation functions A1∼D1 are taken into consideration($n_p = 4$). In the optimaization problem (24) in 2.2, the variables $\gamma_1 \sim \gamma_4$ and the weighting coefficients $c_1 \sim c_4$ are set to be equal all and the weighting coefficients are adjusted so that the strict positive realness condition of $\bar{G}(s)$ in 2.2 is satisfied by the solution K_1. The permissible maximum absolute input values E_{A1}∼E_{D1} to the saturation functions A1∼D1 are obtained as reciprocals of the minimum sector bounds $\alpha_1 \sim \alpha_4$ for 16 groups of control gain matrices and the results are shown in Fig.6. All figure axis labels are shown outside axes on upper side. The following is known from Fig.6: As the effect on DP system stability of actuator servomechanisms in which the saturation function has small E is considered to be significant, the time lags of B/T and S/T propeller pitch servomechanisms affect directly on stability of DP system under wind disturbances from the fore side.

(3)Gain Switching Function

The flowchart of a control gain group selecting logic is shown in Fig.7 in which only the input value ER to A1 saturation function is used as a switching variable monitored by the gain selecting

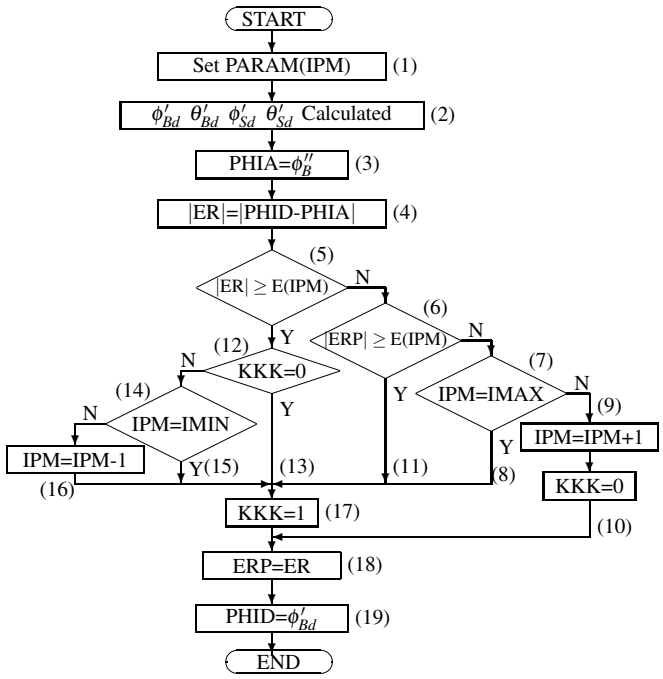

Fig. 7. Logic flow chart of gain selection

logic and when multiple inputs to the saturation functions used as switching variables, OR logic is used in step(5)(6) in Fig.7. The discrete control of control period 1second is used and PARAM(IPM) in step(1) shows the control gain group corresponding to group number IPM which is decided at the previous iteration. PHIA in step(3) indicates the actual value ϕ''_B in the first servomechanism of B/T pitch actuator and PHID in step(4) shows the previous control demand ϕ'_{Bd} in step(19) for B/T pitch as shown in Fig.5. E(IPM) in step(5) shows the permissible maximum absolute input value E_{A1} of A1 function for the control gain group of group number IPM as shown in Fig.6. IMAX and IMIN in step(7) and (14) indicate 16 and 1 respectively. In the controller, firstly the control gain group is selected by IPM which is decided by the previous iteration and the signs of control gain matrices' elements are changed by the quadrant in which the actual thrust vector stays and all control demands are calculated. Secondly the input of A1 function ER=$\phi'_{Bd} - \phi''_B$ is calculated and IPM used for next iteration is decided by the logic in Fig.7.

3.3 Evaluation of Design Method

To evaluate PLC for DP system in which the two inputs to A1 and C1 saturation functions are used as switching variables, the computer simulation using the ship motion nonlinear model shown in the appendix is carried out under the wind velocity U_w change 5m/sec→30m/sec at rising time 0.01sec and wind direction ψ_w=30^o unchanged which is called by disturbance A. The ship is assumed to be initially at rest under the steady wind U_w=5m/sec, ψ_w=30^o. The control performance of DP system by PLC using E_{A1} and E_{C1} in Fig.6 is shown in Fig.8 and the stable time responses are obtained, while the control performance by the ordinary LQ control with fixed gain controller with the largest gain group (IPM=16) is shown in Fig.9 and the settling time in Fig.9 is twice that with PLC in Fig.8. In Fig.8 IPM is decreased from IMAX=16 to 3 at the beginning of control and then IPM is recovered to IMAX=16. The input value of C1 function is negligibly small and so the input value of A1 saturation function as a switching variable is

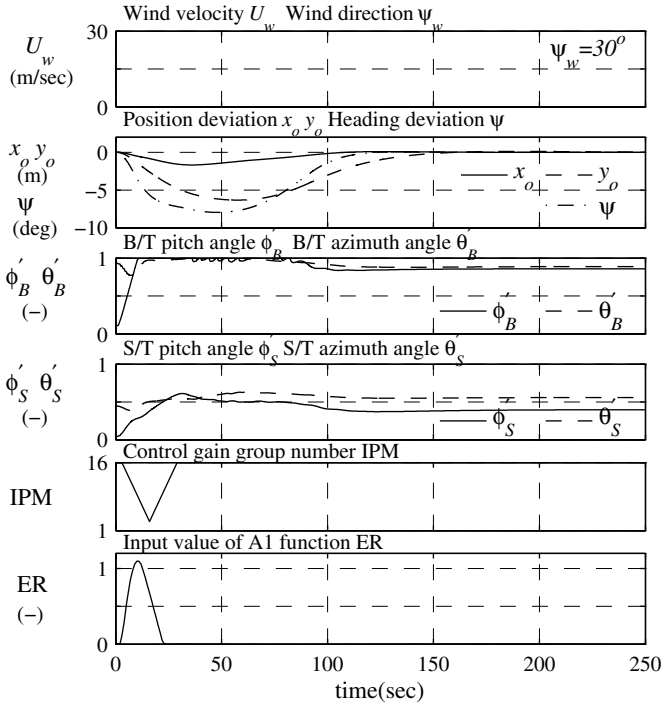

Fig. 8. Time responses by PLC using E_{A1} & E_{C1} in Fig.6 for the disturbance A

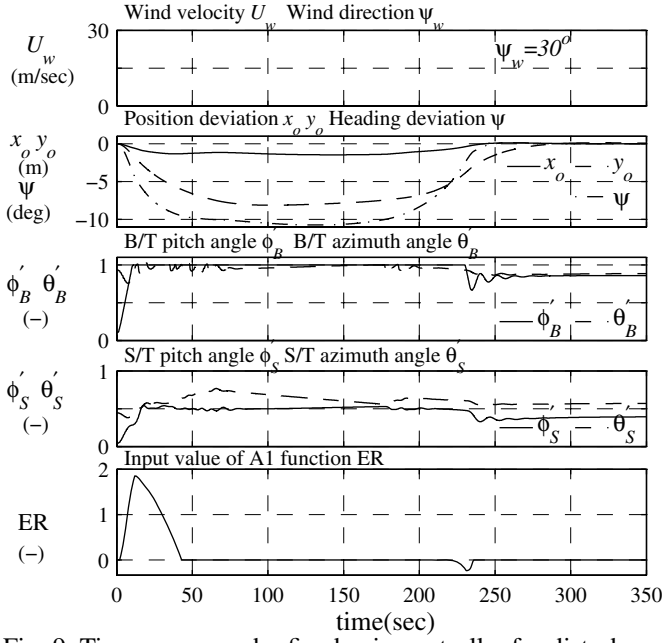

Fig. 9. Time responses by fixed gain controller for disturbance A

effective for PLC of DP system under the disturbance A. In the implementation of the simulation calculation, firstly the B/T pitch angle ϕ''_B in step(3) of the gain selecting logic in Fig.7 has to be obtained by the actuator servomechanism "simulator" which has the same block diagram and receives the same demand from the controller as the actual servomechanism, but whose integrator does not saturate(without a wind-up) because the design method requires the dynamic sytem $G(s)$ in Fig.3 to be linear. If the B/T pitch angle ϕ''_B in the gain selecting logic is obtained from the actual servomechanism with the integrator wind-up, the control performance has more fluctuations in control deviations and actuator responses than those in Fig.8. Secondly as the integral control is used and gain switching of PLC is carried out, it is necessary to use the velocity algorithm

in order that the linearization property holds in Kaminer et al. (1995).

REFERENCES

N. Akasaka. Design of Piecewise Linear LQ Control by Multivariable Circle Criterion for Dynamic Positioning System. *Proc. IECON'2006*, PF-000906, 2006.

F. Blanchini. Survey paper Set invariance in control. *Automatica,35*, pages 1747-1767, 1999.

S. Boyd, L. El Ghaoui, E. Feron and V. Balakrishnan. *Linear Matrix Inequalities in System and Control Theory*, vol.15 of *Studies in Applied Mathematics*. SIAM, Philadelphia, PA, 1994.

C. Edwards and I. Postlethwaite. An anti-windup scheme with closed-loop stability considerations. *Automatica,35*. pages 761-765, 1999.

P. Gahinet, A. Nemirovski, A.J. Laub and M. Chilali. *LMI Control Toolbox*, The MathWorks Inc., Natick, MA, 1995.

H. Hindi and S. Boyd. Analysis of linear systems with saturation using convex optimization. *Proc. 37th Conf. on Decision & Control*, pages 903-908, 1998.

P. Hippe and C. Wurmthaler. Systematic closed-loop design in the presence of input saturations. *Automatica,35*, pages 689-695, 1999.

I. Kaminer, A.M. Pascoal, P.P. Khargonekar and E.E. Coleman. A Velocity Algorithm for the Implementation of Gain-scheduled Controllers. *Automatica,31*(8), pages 1185-1191, 1995.

N. Kapoor, A. Teel and P. Daoutidis. An anti-windup design for linear systems with input saturation. *Automatica,34*(5), pages 559-574, 1998.

H.K. Khalil. *Nonlinear Systems*, Prentice-Hall, Upper Saddle River, NJ, 2002.

T. Kiyama and T. Iwasaki. On the use of multi-loop circle criterion for saturating control synthesis. *Systems Control Lett.,41*, pages 105-114, 2000.

M. Kothare, P. Campo and M. Morari. A unified framework for the study of anti-windup designs. *Automatica,30*(12), pages 1869-1883, 1994.

M.V. Kothare and M. Morari. Multiplier theory for stability analysis of anti-windup control systems. *Automatica,35*, pages 917-928, 1999.

D.A. Lawrence and W.J. Rugh. Gain Scheduling Dynamic Linear Controllers for a Nonlinear Plant. *Automatica,31*(3), pages 381-390, 1995.

T.E. Pare,H. Hindi, J.P. How and S.P. Boyd. Synthesizing Stability Regions for Systems with Saturating Actuators. *Proc. 37th IEEE Conf. on Decision & Control*, pages 1981-1982, 1998.

C. Pittet, S. Tarbouriech and C. Burgat. Stability regions for linear systems with saturating controls via circle and popov criteria. *Proc. 36th Conf. on Decision & Control*, pages 4518-4523, 1997.

W.J. Rugh and J.S. Shamma. Survey Paper Research on gain scheduling. *Automatica,36*, pages 1401-1425, 2000.

G.F. Wredenhagen and P.R. Belanger. Piecewise-linear LQ Control for Systems with Input Constraints. *Automatica,30*(3), pages 403-416, 1994.

Appendix A. PLANAR MOTION EQUATIONS OF A SHIP

Fig.A.1 shows a coordinate axes of a ship motion. Motion equations are shown in the following:

$$
\begin{aligned}
(m+m_x)\dot{u} &= (m+m_y)vr + T_B\cos\theta_B + T_S\cos\theta_S + X_H + X_W,\\
(m+m_y)\dot{v} &= -(m+m_x)ur + T_B\sin\theta_B + T_S\sin\theta_S + Y_H + Y_W,\\
(I_{zz}+J_{zz})\dot{r} &= (m_x-m_y)uv + L_BT_B\sin\theta_B - L_ST_S\sin\theta_S + N_{HW},\\
N_{HW} &= N_H + N_W
\end{aligned}
$$

where (x,y,z):Axes of coordinates fixed to a ship m:Mass of a ship m_x, m_y: Added mass in x- and y-direction I_{zz}, J_{zz}:Mass and added mass moment of inertia of a ship u, v:Ship velocity component in x- and y-direction ψ:Heading of a ship X_H, Y_H, N_H:Hydrodynamic forces in x- and y-direction and moment about z-axis X_W, Y_W, N_W: Wind forces in x- and y-direction and moment about z-axis T_B, T_S:Thrusts of B/T and S/T.

$$
\begin{aligned}
u_a &= \dot{x}_0 = u\cos\psi - v\sin\psi,\\
v_a &= \dot{y}_0 = u\sin\psi + v\cos\psi,\\
r &= \dot{\psi}
\end{aligned}
$$

where (x_0, y_0, z_0):Axes of coordinates fixed in space.

$$
\begin{aligned}
&T_i = \rho n^2 D^4 K_T(J_i,\phi_i) \quad (i=B,S),\\
&K_T(J_i,\phi_i) = K_T(\phi_i) + (\alpha_T\phi_i + \alpha_C)J_i \quad (i=B,S),\\
&J_B = (1-w)(u_s\cos\theta_B + v_s\sin\theta_B + L_Br\sin\theta_B)/(nD),\\
&J_S = (1-w)(u_s\cos\theta_S + v_s\sin\theta_S - L_Sr\sin\theta_S)/(nD),\\
&u_s = u + U_c\cos(\psi_c-\psi), \quad v_s = v + U_c\sin(\psi_c-\psi)
\end{aligned}
$$

where ρ:density of sea water n:revolution speed of thrusters D:Thruster diameter K_T: Thrust coefficient in bollard pull condition J_B, J_S:Advance coefficient at thrusters' location w:Wake coefficient α_T, α_C:Correction factors of K_T U_c: Current velocity ψ_c:Current direction L_B, L_C:thrusters' locations.

$$
\begin{aligned}
&X_H = X_c(\beta)\rho\nabla^{\frac{2}{3}}V_s^2/2, \quad Y_H = Y_c(\beta)\rho\nabla^{\frac{2}{3}}V_s^2/2,\\
&N_H = N_c(\beta)\rho\nabla^{\frac{2}{3}}L_{pp}V_s^2/2,\\
&\beta = \tan^{-1}(v_s/u_s), \quad V_s^2 = u_s^2 + v_s^2
\end{aligned}
$$

where $X_c(\beta), Y_c(\beta), N_c(\beta)$:Coefficient functions of attack angle β for hydrodynamic forces and moment L_{pp}:Length of a ship ∇: Capacity.

$$
\begin{aligned}
&X_W = C_X(\beta_w)\rho_a A_{AT}V_w^2/2, \quad Y_W = C_Y(\beta_w)\rho_a A_{AL}V_w^2/2,\\
&N_W = C_N(\beta_w)\rho_a L_{pp}A_{AL}V_w^2/2,\\
&u_w = u + U_w\cos(\psi_w-\psi), \quad v_w = v + U_w\sin(\psi_w-\psi),\\
&\beta_w = \tan^{-1}(v_w/u_w), \quad V_w^2 = u_w^2 + v_w^2
\end{aligned}
$$

where ρ_a:density of air A_{AT}:Longitudinal projected area of a ship body above water line A_{AL}:Lateral projected area of a ship body above water line $C_X(\beta_w), C_Y(\beta_w), C_N(\beta_w)$:Coefficient functions of wind attack angle β_w U_w:Wind velocity ψ_w:Wind direction.

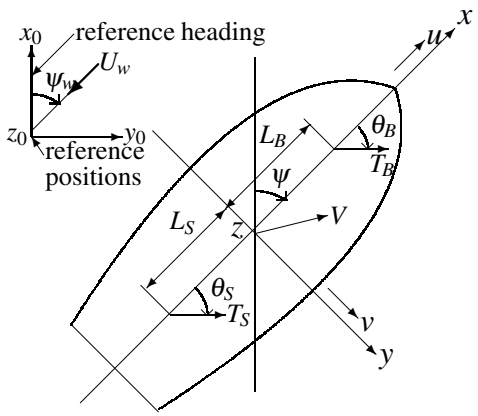

Fig. A.1. Coordinate axes of a ship motion